ICONHIC2019
2nd International Conference on Natural Hazards & Infrastructure
23-26 June, 2019, Chania, Greece

Towards a tsunami nonlinear static analysis procedure for the ASCE 7 standard

M. Baiguera[1], T. Rossetto
University College London, UK

I.N. Robertson
University of Hawai'i at Mānoa, HI, USA

C. Petrone
Willis Tower Watson, UK

ABSTRACT

Tsunami design provisions for coastal structures are now included in a new chapter of ASCE 7-16 Standard. The provisions provide prescriptive tsunami loading and design requirements, and they allow for the use of alternative performance-based criteria, including nonlinear static analysis. However, no guidance is provided as to how the performance-based analysis should be performed. This paper presents an improved nonlinear static pushover procedure for the assessment of the nonlinear capacity of structures to tsunami, within the framework of the ASCE 7-16 provisions. For this purpose, a prototypical reinforced concrete multi-storey building exposed to high seismic and tsunami hazards along the Northwest Pacific coast of the USA is assessed. Two different tsunami load discretisation methods are applied to investigate the structural capacity under tsunami systemic and component loading, respectively. The results of the nonlinear static pushover analyses show that the structural system has sufficient lateral strength to resist ASCE 7-16 prescribed tsunami loads. However, when component-based loading is considered, the seaward ground storey columns are observed to fail in shear, precipitating structural failure. Overall, the nonlinear static pushover analysis, considering component behaviour, provide the same result as the ASCE 7-16 simplified systemic acceptance criteria, i.e. that the structure is unsafe for use as a refuge, and that it would require significant strengthening.

Keywords: Tsunami Engineering, Concrete frames, Tsunami Pushover, ASCE 7 Standard

INTRODUCTION

The catastrophic effects of recent tsunamis in the Indian Ocean (2004), Chile (2010), Japan (2011), and Indonesia (2018) have highlighted the threat that earthquake-triggered tsunamis pose to coastal areas. Many communities along the Pacific coast of the United States are exposed to this rare but extreme hazard. It has been established that the Pacific Northwest coast has the potential of being hit by a devastating tsunami following a M_w 9 earthquake generated along the Cascadia subduction zone (*Atwater et al., 1991; Yeats, 2015; Goldfinger et al., 2017*).

[1] Corresponding Author: M. Baiguera, University College London, *m.baiguera@ucl.ac.uk*

To increase the disaster resilience of coastal areas and mitigate tsunami damage to structures, tsunami design procedures are now included in US design codes through the introduction of a new Chapter 6, Tsunami Loads and Effects, in ASCE 7-16, *Minimum Design Loads and Associated Criteria for Buildings and Other Structures* (*ASCE, 2017*). *Robertson (2019)* provides extensive explanation and example applications of the ASCE 7-16 tsunami design provisions. These provisions, which are included in the requirements of the 2018 International Building Code (IBC), provide prescriptive loading and design requirements for tsunami effects on buildings and other structures within the mapped Tsunami Design Zone (TDZ). For instance, it is assumed that a building designed for ASCE 7-16 seismic design category D, E or F (high seismic) can resist the maximum considered tsunami (MCT, 2% probability of exceedance in 50 years) when the corresponding overall tsunami force is less than 75% of the overall lateral seismic resistance of the structural system, considering overstrength. *Carden et al. (2015)* and *Chock et al. (2018)* used this approach for a preliminary study aimed at comparing the tsunami resistance of prototypical reinforced concrete and steel structures located in high seismicity areas in US and Japan. In addition, this study was the basis for the recommended height thresholds for multi-storey buildings to meet life safety performance. However, this assessment technique is solely based on the code seismic and tsunami design requirements, which typically derive from conservative assumptions. As an alternative to prescriptive provisions, the code allows for the use of performance-based criteria, which include nonlinear static analysis. However, no detailed guidance is provided as to how these performance-based methods should be performed.

Design and assessment performance-based methodologies of structures to tsunami are much less developed than those available for other natural hazards, such as earthquakes. For instance, in seismic engineering, nonlinear static and dynamic analysis, generally referred to as pushover analysis and time-history analysis, respectively, are well-established tools for performance-based design and assessment of structures. In the case of tsunami, the lack of understanding of the complex nature of onshore inundation processes, particularly the flow interaction with buildings, has hampered the development of analytical methods *(Rossetto et al. 2018).* Recently, field observations from tsunami reconnaissance missions, combined with advances in physical modelling in laboratories, have led to a limited number of studies that have established new analysis tools, often combined with enhanced relationships for estimating tsunami loading. *Macabuag et al. (2014)* developed a sensitivity study to compare the structural response of a simple reinforced concrete frame under different code-based tsunami loadings, including those prescribed by ASCE 7-16. Pushover analyses were performed using a nonlinear finite element model where the hydrostatic or hydrodynamic force was distributed along the seaward columns. For instance, the hydrodynamic lateral forces corresponding to a given inundation depth were applied at each storey level and monotonically increased up to the maximum force, i.e. assigning a constant inundation depth during the analysis. This approach is herein referred to as constant depth pushover (CDPO). *Attary et al. (2017)* performed CDPO analyses in a fragility assessment of a low-rise steel moment frame. Random sets of tsunami depth and flow velocity values were used to generate a suite of tsunami forces, which were estimated based on FEMA P-646 (*FEMA, 2012*) guidelines and applied at each storey level. *Alam et al. (2018)* used a similar approach for the fragility assessment of a six-story reinforced concrete (RC) school. The analysis approach was enhanced by introducing distributed loading along the vertical structural members and by explicitly accounting for shear failure of columns. The hydrodynamic tsunami force was estimated based on the ASCE 7-16 Standard provisions. Since no specific building location along US coast was selected, CDPO analyses were performed using a random suite of inundation depth and velocity. In the context of tsunami fragility assessment of RC buildings, *Petrone et al. (2017)* developed novel analysis approaches, namely time-history dynamic analysis and variable height pushover. The latter is referred to in this paper as variable depth pushover (VDPO). The tsunami time-history procedure follows the same principles of a seismic time-history analysis, apart from the input data, which is the tsunami force estimated from a simulated inundation time-history. In a VDPO, the tsunami inundation depth at the site of the structure monotonically increases, while the flow velocity is calculated assuming a constant Froude number. For all methods, the estimation of the tsunami hydrodynamic force was based on experimentally-validated equations by *Qi et al, (2014),* which account for the regime conditions of the flow impacting the structure and the density of the urban environment. In *Petrone et al. (2017),* comparison of the results of time-history, VDPO analysis and CDPO analysis highlight that, in terms of engineering demand parameters, (i.e. inter-storey drifts and column shear forces), VDPO is in good agreement with the dynamic analysis, and consistently more accurate than CDPO.

This paper presents the preliminary stage of a study aimed to develop tsunami nonlinear static pushover analysis procedures that are compatible with the provisions of the ASCE 7-16 Standard. In particular, an

improved VDPO approach is proposed that is capable of reproducing the post-peak behaviour of the structure under tsunami loading. The improved VDPO is adopted in the systemic response assessment of a prototypical RC frame in a TDZ, using different loading assumptions. The results of this assessment are compared to the prescriptive acceptance criteria of the ASCE 7-16 provisions.

METHODOLOGY

Case study building

A case study building is used in this paper to compare the systemic response calculated using VDPO and the ASCE 7-16 prescriptive acceptance criteria. A six-storey office building consisting of RC special moment resisting frames (SMRF), a flat plate post-tensioned concrete floor system, and interior gravity load columns, is chosen as the case study. The building is located in Seaside, Oregon, which is exposed to high seismic and tsunami hazards due to the Cascadia subduction zone. Fig. 1 shows the floor plan and section for this building. The case study building was initially designed for the ASCE 7 specified wind and seismic conditions at Monterey, California (*Yokoyama and Robertson, 2014*). The building lateral force resisting system consists of four moment resisting frames in the narrow direction (also the assumed tsunami flow direction) and two moment resisting frames in the wide direction (Fig. 1). Because of the similarity in seismic hazard at Seaside and Monterey, the same building design is appropriate for both locations. Soil classification D for stiff soil is assumed for the building site. The size of the columns is uniform along the height of the building, i.e. 71.1x71.1 cm for the SMRFs, and 61x61 cm for the internal gravity load columns, while the size of beams is 76.2 wide by 61 cm deep. The concrete cover is 5 cm. In the SMRF columns, steel reinforcing ratio varies from 1.3% at the ground floor to 1% at the upper stories. Transverse reinforcement in the SMRF columns consists of ties with three 9.5-mm-diameter legs at every 10 cm in the column ends (71 cm long) and every 15 cm in the central section. More details about the seismic design of the building are provided in *Yokoyama and Robertson (2014)*. Complete tsunami design examples for this building and others located at Monterey, Hilo and Waikiki are provided in *McKamey and Robertson (2019).*

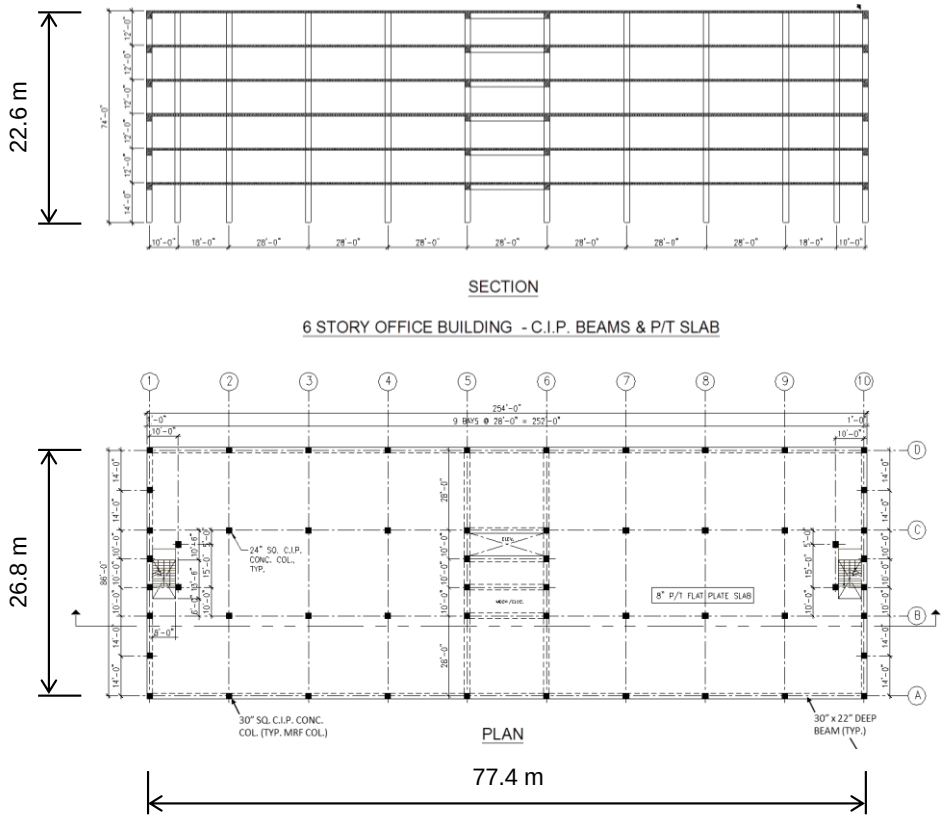

Figure 1. Prototype building (*Yokoyama and Robertson, 2014*)

Table 1. Prototype building location, associated design wind speeds and seismic design criteria per ASCE 7

	Latitude	Longitude	Design Wind Speed	Site Class	Seismic Design Category	S_S	S_1	S_{DS}	S_{D1}
Monterey, CA	36.6002 N	121.8818 W	110	D	D	1.513g	0.554g	1.009g	0.554g
Seaside, OR	45.9947 N	123.9294 W	110	D	D	1.332g	0.683g	0.888g	0.683g

Tsunami loading

The case study building location is near the coastline and falls within the 2,500-year probabilistic tsunami design zone map of Seaside, as illustrated in Fig. 3. Designated as an office building, the structure is classified as Tsunami Risk Category (TRC) II, and therefore it is not subject to tsunami provisions. However, tall TRC II buildings can be designated by local jurisdictions to provide effective secondary alternative refuge, provided that their height exceeds a certain local threshold. *Chock et al. (2018)* established suitable height thresholds for communities throughout the US Pacific coast, satisfying both the lateral force resisting system capacity (described in the 'Results' section) and a recommended height at least 3.66 m greater than the inundation depth.

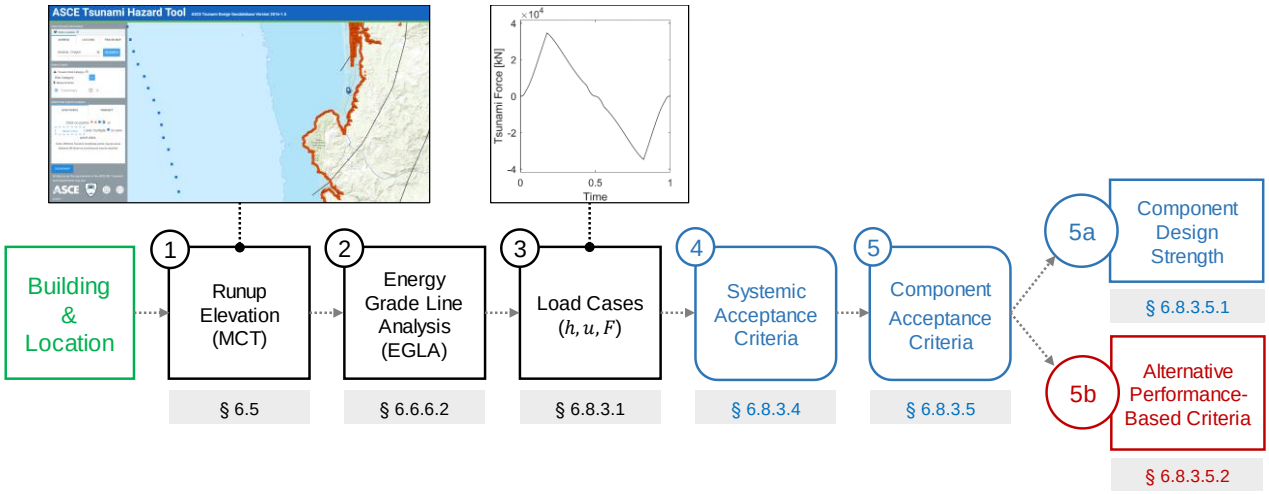

Figure 2. ASCE 7-16 tsunami design methodology

The ASCE 7-16 provisions provide a practical methodology to calculate the overall tsunami load on a structure. Fig. 2 illustrates a summary of the main steps of the design procedure for buildings in TRC II or III. The maximum inundation depth h_{max} and flow velocity u_{max} at the building site are determined by applying the Energy Grade Line analysis (*Kriebel et al., 2017*). As shown in Fig. 3, the appropriate two-dimensional topographic transect and runup elevation are determined from the 2500-year TDZ maps provided in the ASCE Tsunami Geodatabase. As a result, for the Seaside prototype building site, h_{max} and u_{max} are 9.57 m and 11.56 m/s, respectively *(McKamey & Robertson, 2019)*. This indicates that the upper three stories of the building could function as a refuge, according to the proposal of *Chock et al. (2018)*. The code provisions provide normalised inundation depth (h/h_{max}) and flow velocity (u/u_{max}) time-histories that are intended to describe all possible combinations of depth and flow during the tsunami inundation. These are used in this paper to determine the maximum design structural loading for the building, as shown in Fig. 4.

The overall lateral force on a structure (F_T) is estimated using the following hydrodynamic drag equation *(ASCE, 2017)*:

$$F_T = 0.5\rho_s I_{tsu} C_d C_{cx} B(hu^2) \quad (1)$$

where ρ_s is the fluid mass density, I_{tsu} is the importance factor for tsunami forces (= 1.0 for TRC II), C_d is the drag coefficient based on the ratio B/h [Table 6.10-1 in *ASCE (2017)*], C_{cx} is the proportional closure coefficient (with a minimum value of 0.7, adopted in this study), B is the building width, h is the inundation

depth, and u is the flow velocity. As shown in Fig. 4, the maximum lateral hydrodynamic force on the structure occurs at the peak velocity in each direction, when the inundation depth is 2/3 of h_{max}. This is the most critical stage that is indicated as Load Case 2 (LC2) in the provisions.

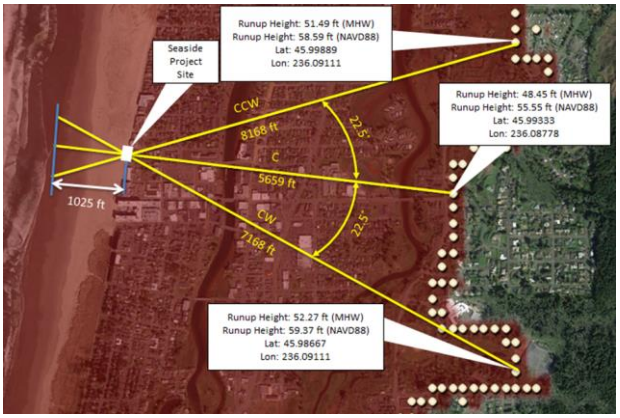

Figure 3. Energy Grade Line Analysis at building site in Seaside (*McKamey & Robertson, 2019*)

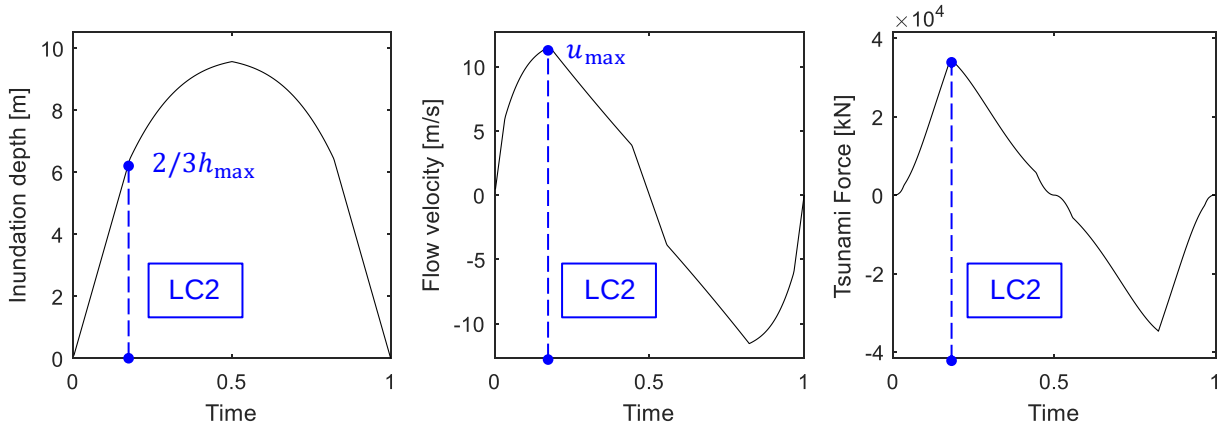

Figure 4. Tsunami inundation depth, flow velocity and force time-histories for the building site

Finite element model

The case study building is modelled in OpenSees (*McKenna et al. 2013*) as a two-dimensional model replicating one half of the full structure. As illustrated in Fig. 5, this model includes one end moment resisting frame (with 8 column), one interior moment resisting frame (with 6 columns), six exterior columns that form part of the transverse exterior moment resisting frames, and six internal gravity columns. All these components are linked by means of master-slave node control so as to simulate a rigid diaphragm at each floor level.

The OpenSees model uses force-based nonlinear beam-column elements to model columns and beams. A distributed plasticity model is adopted, since the inelastic behaviour due to tsunami pressure can form at any point along the column height. A fibre approach is used for the cross-sections with five integration points along each element. The integration along the element is based on Gauss-Lobatto quadrature rule (two integration points at the elements ends). Concrete within the reinforcement cage is associated with a confined concrete constitutive law, while the cover concrete outside the reinforcement cage is modelled as unconfined concrete.

The concrete used in the prototypical building design has a nominal compressive strength of 27.6 MPa, while the reinforcing steel has a nominal yield strength f_y = 414 MPa. Based on ASCE 41-13 Table 10-1 *(ASCE, 2014)*, the concrete compressive strength should be multiplied by 1.5 to obtain a realistic in-situ compressive strength, i.e. 41.4 MPa. Similarly, the steel yield strength is anticipated to be 1.25 times the specified yield strength of the steel, i.e. 517 MPa, while the tensile strength is also anticipated to be 1.25 times the actual tensile strength. Assuming a strain hardening ratio of 1.5, this results in a realistic tensile strength of 776 MPa. The constitutive material model by *Mander et al. (1988)*, referred to as *Concrete04* in OpenSees, is employed for confined and unconfined concrete in column and beam cross-sections. It is noted that the *Concrete04* model simulates stiffness degradation. The steel stress-strain constitutive material is modelled using the Giuffre-

Menegotto-Pinto model, named as *Steel02* in OpenSees. Reinforcing steel is assumed to have a strain hardening of 0.004 and an ultimate steel strain of 0.3.

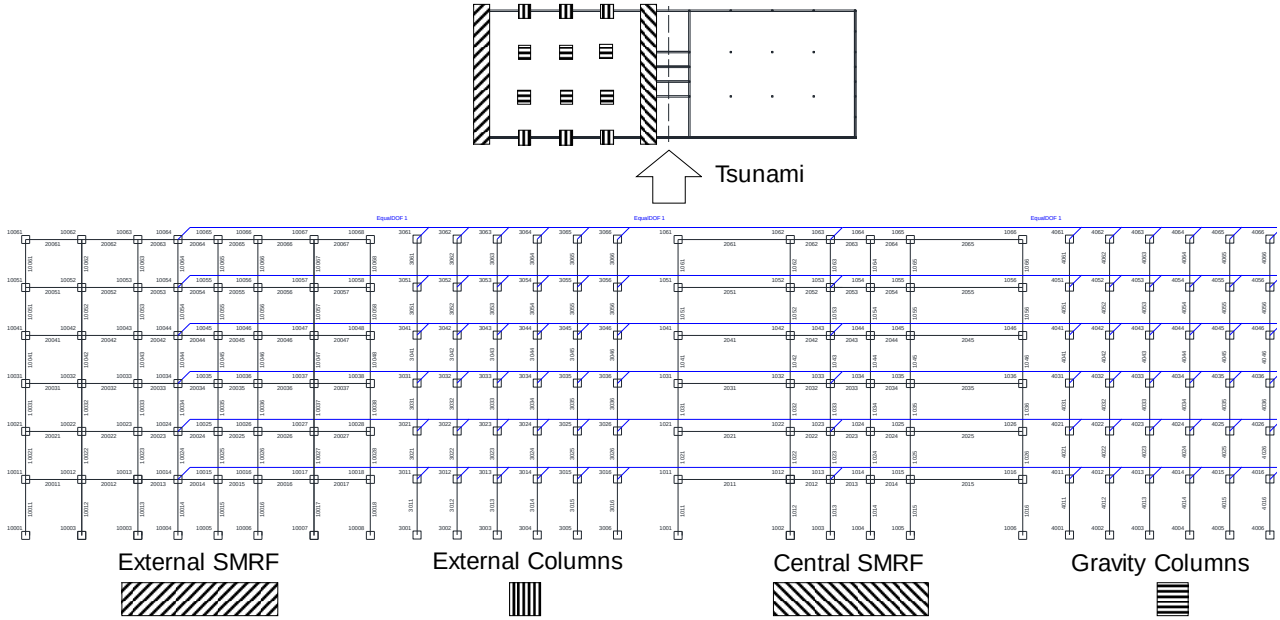

Figure 5. Finite element model of half of the full prototypical building

Nonlinear Pushover Analysis Procedure

The design methodology of the ASCE 7-16 code provisions, illustrated in Fig. 2, allows for the use of alternative performance-based criteria to check the design of structural components. This includes the adaptation of nonlinear static pushover analysis of ASCE 41-13 *(ASCE, 2014)* to tsunami loading. The objective of this paper is to develop a procedure whereby nonlinear static pushover analysis can be applied for tsunami assessment of buildings located in the TDZ, following the ASCE 7-16 provisions.

Analysis procedure

An improved nonlinear static analysis based on the methodologies proposed in *Petrone et al. (2017)*, is developed to analyse the prototypical building. This consists of a two-phase analysis procedure. In Phase 1, a force-controlled pushover analysis is conducted assuming an inundation depth that increases at each time-step. In Phase 2, the analysis switches to displacement-control, where the displacement is incremented, and the corresponding tsunami force is calculated assuming the same inundation depth (and load pattern) as in the last step of Phase 1 of the analysis. The switch from Phase 1 to 2 occurs at the end of the force-controlled phase (as defined by the user) or when the analysis encounters a numerical convergence issue. In the latter case, the Phase 1 analysis is repeated up to the time step preceding the numerical issue, and then Phase 2 is initiated. This new VDPO approach provides an improved ability to capture the post-peak response of the structure as compared to the approach proposed in *Petrone et al. (2017)*, (i.e. a purely force-controlled analysis).

For the application of the improved VDPO in this paper, Phase 1 applies a tsunami force in accordance with the ASCE 7-16 inundation depth and flow time histories up to LC2. Throughout Phase 1 and 2 of the analysis, the tsunami hydrodynamic force on the structure is estimated according to Equation 1, which accounts for a varying C_d dependent on B/h, as illustrated in Fig. 6.

As highlighted in previous studies *(Petrone et al., 2017; Alam et al., 2018)*, the occurrence of shear failure of columns is a typical collapse mechanism under tsunami loading, often precipitating global failure if no strengthening measures are adopted. In this study, shear failure occurrence is tracked in all first-storey columns (i.e. those subjected to the highest shear demand), according to the formulation used in ASCE 41-13. It is noted that, both the end and central column sections (Sections E and C, in Fig. 8, respectively), are checked due to differences in their shear reinforcement.

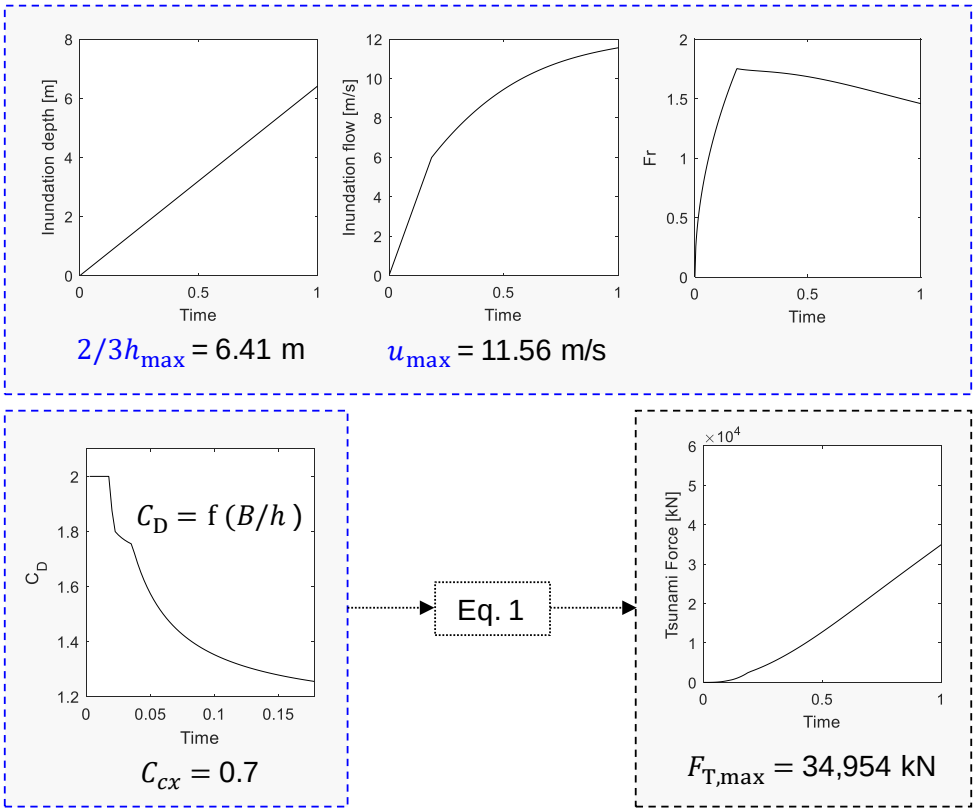

Figure 6. Phase 1 of the VDPO: Calculation of overall tsunami force on the structure (Equation 1) up to LC2.

Load discretisation methodologies

ASCE 7-16 provisions assume that the hydrodynamic load pressure distribution on the building is uniform. Recently, *Petrone et al. (2017)* have used linear or trapezoidal load distributions, as experimental evidence shows that tsunami loading under steady flow conditions is similar to hydrostatic pressure distribution *(Lloyd, 2016)*. It is noted that a comparison between uniform and linear/trapezoidal load distributions is not addressed in this preliminary work. A load sensitivity analysis carried out in *Petrone et al. (2017)* illustrates different methods that can be applied for distributing the hydrodynamic load pressure over the height of the building. The simplest approach (named here as S) is to apply the loads at each storey level: the tsunami forces are calculated using a simple influence area approach, as illustrated in Fig. 7 (left). This is a typical approach used in past studies and is in agreement with the code provisions. An alternative approach (D) is to allocate a portion of the total base shear directly to each of the five SMRF columns on the front of the building. In this case, the lateral load is applied at 6 points along each column height (see Fig. 7 right). This load discretisation is the one recommended in *Petrone et al. (2017)*, which they show to provide the best estimation of demand parameters.

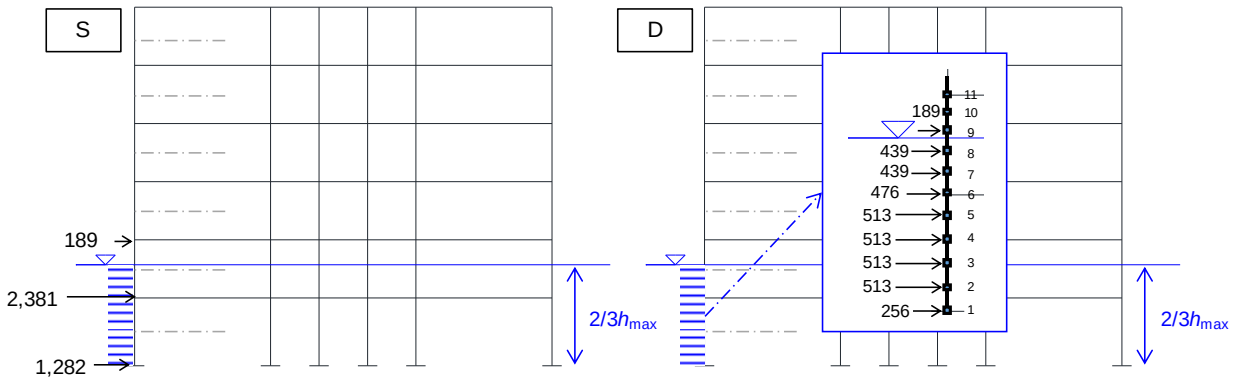

Figure 7. Loading discretisation methods S (left) and D (right) for the central SMRF central (see Fig. 5 for frame location; similar distributions are applied to the other 4 columns on the leading edge of the building; all forces for LC2 in kN)

RESULTS

Prescriptive systemic acceptance criterion

ASCE 7-16 provides a simple criterion to evaluate the systemic tsunami capacity of a seismically-designed structure. This assumes that a building designed to resist high seismic loading (i.e. Seismic Design Criteria D, E or F), has sufficient inherent strength to resist the tsunami force *(Chock et al., 2018)*. Effectively, this implies that structural lateral force resisting system does not require additional lateral strength when:

$$F_T < 0.75\Omega_0 E_h \quad (2)$$

where Ω_0 is the system seismic overstrength factor, and E_h is the effect of horizontal earthquake forces. From the design of the prototypical building ($\Omega_0 = 3$ for special MRFs, based on ASCE 7 Table 12.2-1), $\Omega_0 E_h$ = 30,123 kN. Given that the applied tsunami force F_T = 34,954 kN at LC2 as per Equation 1 (see Fig. 7), the systemic acceptance criterion described in Equation 2 is not met. The seismic lateral force resisting system would need to be strengthened so as to meet this criterion.

Nonlinear pushover analysis

The lateral capacity of the structure to resist tsunami loads is evaluated using the improved VDPO. To draw a consistent comparison between the actual lateral tsunami capacity with the corresponding seismic one, a seismic pushover analysis is also performed. The fundamental period of the model is 0.8 s, and the first mode is characterised by 83% mass participation factor. The seismic pushover is conducted using a lateral load distribution corresponding to the first mode response.

Fig. 8 compares the total base shear-top drift curve from the seismic pushover analysis with the one from the VDPO with discretisation method S (top) and D (bottom). It can be seen from the seismic pushovers that the actual seismic lateral capacity (16,839 kN) is significantly larger than the design one (10,041 kN), however, it is substantially less than that predicted by the use of an overstrength factor $\Omega_0 = 3$ (30,123 kN).

In the case of the tsunami VDPO, for both S and D loading conditions, the systemic tsunami capacity of the building is significantly larger than the overall tsunami at LC2 (F_T = 34, 954 kN, shown as a thick dashed line in Fig. 8). This assessment contradicts the results of the simplified ASCE 7-16 systemic tsunami capacity acceptance criterion, and would indicate that the structure is safe for use as a refuge without additional strengthening.

However, ASCE 7-16 also requires that every structural element be evaluated for component loads. For exterior columns, such as the SMRF columns in this building, the component loads include hydrodynamic drag with debris damming effects, and debris impact loading. The member forces resulting from these component loads must be added to the member forces resulting from the systemic loads, and the member designed for the combined loading using the conventional strength design approach.
Loading discretisation D can be assumed as a proxy for applying the combined systemic and component loads to the seawards columns (Fig. 8, bottom). In fact, this load discretisation is seen to result in a very slightly reduced overall tsunami capacity. However, the seaward columns experience larger shear forces, more akin to the requirements for added component loading of ASCE 7-16. In reality, when the ASCE 7-16 component loading criteria are applied to each single column, the imposed local forces will be even larger than those seen here for load discretisation case D. This will be addressed in future publications.

The OpenSees model does not evaluate shear failure, so a separate shear check was performed on all columns post-analysis. For discretisation method S, there are no shear failures in the first floor columns. However, in discretisation D, where the lateral load is applied directly to the seaward columns, column shear failure is seen to occur, as noted in Fig. 8 (bottom). The external SMRF columns (located between the two transverse SMRFs, as illustrated in Fig. 5) are actually observed to be the first columns to fail in shear (preceding the shear failure of the other seaward columns). Interestingly, these fail in shear in their central sections (i.e. where the transverse reinforcement spacing is wider) at F_T = 17,903 kN, indicating component failure results in a premature failure of the structure.

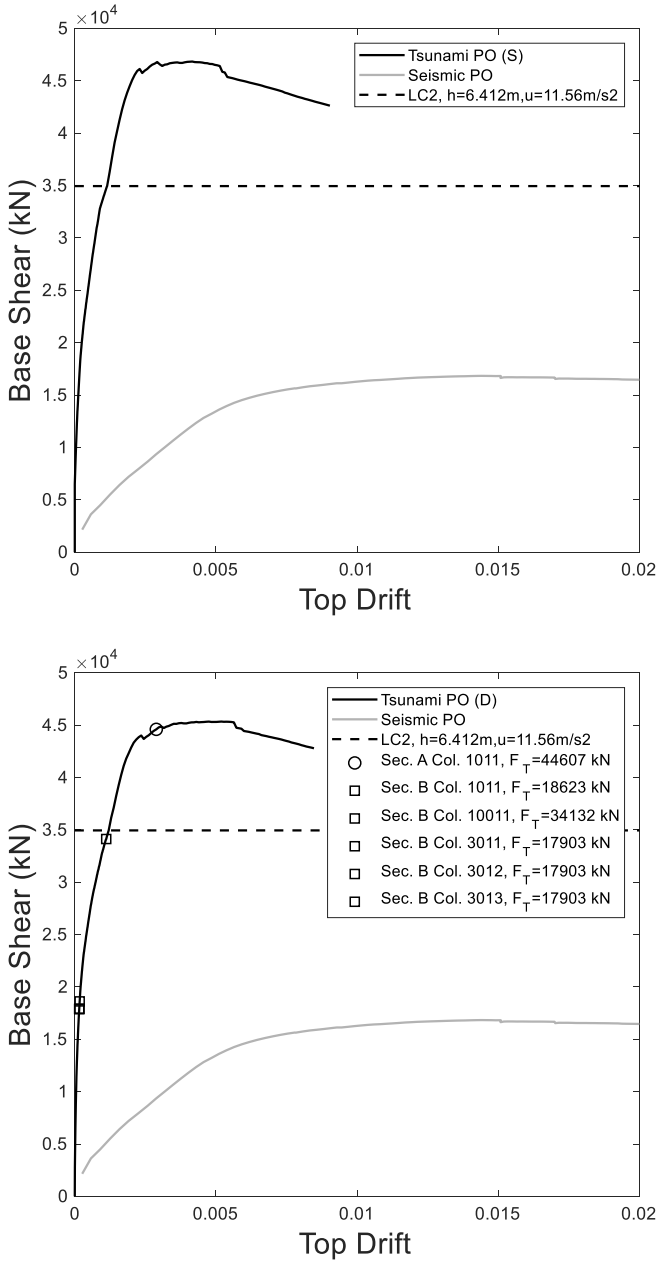

Figure 8. Base shear-top drift curves from seismic PO analysis and tsunami PO with storey-level load discretisation methods: (top) S; and (bottom) D

If shear failure of the first column is assumed as the structural failure criterion, this reduced capacity is almost half the ASCE 7-16 tsunami load (F_T = 34,954 kN). This analysis results in the same conclusions as the simplified ASCE 7-16 systemic tsunami capacity acceptance criterion, i.e. that the structure is not safe for use as a refuge without additional strengthening. However, the use of the VDPO also provides information of what needs to be strengthened in order to improve the tsunami performance of the structure, i.e. the shear strength of the ground floor seaward columns, in this example case.

CONCLUSIONS

New tsunami design provisions in ASCE 7-16 Chapter 6 offer a practical methodology for the design of buildings to tsunami. While the use of performance-based analysis tools is permitted, no specific guidance is provided. This study presents an improved variable depth pushover analysis approach (VDPO) for the assessment of the non-linear capacity of structures subjected to tsunami. The results of using the VDPO are compared to the simplified ASCE 7-16 systemic tsunami capacity acceptance criterion for a case study RC

frame located in a high tsunami hazard area. The systemic response of the structure was investigated using VDPO, applying two different tsunami load discretisation methods. For both load discretisation cases, the tsunami systemic capacity of the structure was seen to be sufficient to resist the ASCE 7-16 prescribed tsunami loads. However, when component-based loading was considered, the seaward ground storey columns were observed to fail in shear, precipitating structural failure. Overall, the VDPO analysis, considering component behaviour, provided the same result as the ASCE 7-16 simplified systemic acceptance criteria, i.e. that the structure was unsafe for use as a refuge, and that it would require significant strengthening. However, based on this example alone, it is not possible to say whether the simplified ASCE 7-16 systemic tsunami capacity acceptance criterion is safe or unsafe. As far as the authors understand, the criterion does not capture the significantly different nature of the pushover response of the structure under seismic and tsunami loading. Hence, further investigations are required to ascertain the conservatism of the simplified approach, considering other designs of structures and more locations along the US Pacific Coast with different combinations of seismic and tsunami hazard. In addition, the effect of the preceding earthquake will be addressed in a separate stage of this research work.

ACKNOWLEDGMENTS

The research work presented in this paper is funded by the European Research Council, ERC grant agreement 336084 URBANWAVES (awarded to Professor Tiziana Rossetto). The authors are grateful to Mr. Gary Chock (President, Martin&Chock; Chair, ASCE 7 Tsunami Loads and Effects Subcommittee), Dr. Lyle Carden (Principal, Martin&Chock), and Mr. Jacob McKamey for their assistance in this research.

REFERENCES

Alam M.S., Barbosa A.R., Scott M.H., Cox D.T., van de Lindt J.W. Development of Physics-Based Tsunami Fragility Functions Considering Structural Member Failures. Journal of Structural Engineering, 144(3), 04017221.

ASCE (2014). Seismic Evaluation and Retrofit of Existing Buildings. ASCE/SEI 41-13, Reston, VA, USA.

ASCE (2017). Minimum Design Loads and Associated Criteria for Buildings and Other Structures. ASCE/SEI 7-16. Reston, VA, USA.

Attary N., Unnikrishnan V.U., van de Lindt J.W., Cox D.T., Barbosa A.R. (2017). Performance-Based Tsunami Engineering Methodology for Risk Assessment of Structures. Engineering Structures, 141, 676–686.

Atwater B.F., Stuivert M., Yamaguchi D.K. (1991). Radiocarbon Test of Earthquake Magnitude at the Cascadia Subduction Zone. Nature, 353, pp. 156–158.

Carden L., Chock G., Robertson I.N. (2015). The New ASCE Tsunami Design Standard Applied to Mitigate Tohoku Tsunami Building Structural Failure Mechanisms. Chap. 22 In Handbook of Coastal Disaster Mitigation for Engineers and Planners, edited by M. Esteban, H. Takagi, and T. Shibayama. Oxford, UK.

Chock G.Y., Carden L., Robertson I.N., Wei Y., Wilson R., Hooper J. (2018). Tsunami-Resilient Building Design Considerations for Coastal Communities of Washington, Oregon, and California. Journal of Structural Engineering, 144(8), 04018116.

FEMA (2012). Guidelines for Design of Structures for Vertical Evacuation from Tsunamis. FEMA P-646. Washington, DC.

Goldfinger C., Galer S., Beeson J., Hamilton T., Black B., Romsos C., Patton J., Nelson C.H., Hausmann R., Morey A. (2017). The Importance of Site Selection, Sediment Supply, and Hydrodynamics: A Case Study of Submarine Paleoseismology on the Northern Cascadia Margin, Washington USA. Marine Geology, 384, pp. 4–46.

Kriebel D.L., Lynett P.J., Cox D.T., Petroff C.M., Riggs H.R., Robertson I.N., Chock, G.Y.K. (2017). Energy Method for Approximating Overland Tsunami Flows. Journal of Waterway, Port, Coastal, and Ocean Engineering 143(5).

Lloyd T.O. (2016). An Experimental Investigation of Tsunami Forces on Coastal Structures. PhD Thesis, University College London, London.

Macabuag J., Lloyd T., Rossetto T. (2014). Sensitivity Analyses of a Framed Structure under Several Tsunami Design-Guidance Loading Regimes. In Second European Conference on Earthquake Engineering and Seismology. Istanbul.

Mander J.B., Priestley M.J.N., Park R. (1988). Theoretical Stress-Strain Model for Confined Concrete. Journal of Structural Engineering, 114(8), pp. 1804–1826.

McKamey, J. and Robertson, I.N., (2019). Cost Implications for Including Tsunami Design in Mid-Rise Buildings along the US Pacific Coast. Research Report, University of Hawaii at Manoa, UHM/CEE/19-01.

McKenna F. & Fenves G. (2013). OpenSees Manual. Berkeley, California. Available at: http://opensees.berkeley.edu.

Petrone C., Rossetto T., and Goda K. (2017). Fragility Assessment of a RC Structure under Tsunami Actions Via Nonlinear Static and Dynamic Analyses. Engineering Structures, 136, pp. 36–53.

Qi Z.X., Eames I., Johnson E.R. (2014). Force Acting on a Square Cylinder Fixed in a Free-Surface Channel Flow. Journal of Fluid Mechanics, 756, pp. 716–727.

Robertson I.N. (2019). Tsunami Loads and Effects: Guide to the Tsunami Design Provisions of ASCE 7-16. ASCE Publications.

Rossetto T., Petrone C., Eames I., De La Barra C., Foster A., Macabuag J. (2018). Advances in the Assessment of Buildings Subjected to Earthquakes and Tsunami. In: Pitilakis K. (eds) Recent Advances in Earthquake Engineering in Europe. ECEE 2018. Thessaloniki, Greece.

Yeats R. (2015). Earthquake Time Bombs. Cambridge University Press.

Yokoyama J. & Robertson I.N. (2014). Evaluation of Reinforced Concrete Buildings when Subjected to Tsunami Loads. Research Report, University of Hawaii at Manoa, UHM/CEE/14-01.